THE JOURNAL OF PHYSICAL CHEMISTRY A

Article

pubs.acs.org/JPCA

Electrical Phenomena of Soft Particles. A Soft Step Function Model

Hiroyuki Ohshima*

Faculty of Pharmaceutical Sciences, Tokyo University of Science, 2641 Yamazaki, Noda, Chiba 278-8510, Japan, and Center for Colloid and Interface Science, Research Institute for Science and Technology, Tokyo University of Science, 2641 Yamazaki, Noda, Chiba 278-8510, Japan

ABSTRACT: Simple analytic expressions are derived for the electrophoretic mobility of a soft particle consisting of the hard particle core covered with an ion-penetrable surface layer of polyelectrolyte for the case where the electric potential is low. The effect of the distribution of the polymer segments is taken into account by modeling the surface layer as a soft step function with the inhomogeneous distribution width δ. It is shown that the electrophoretic mobility becomes lower than that for the hard step function model and that the maximum deviation of the soft step function model from the hard step function model, which is a function of $\lambda\delta$ (where $1/\lambda$ is the softness parameter) and κ/λ (κ is the Debye–Hückel parameter), is 2.7% at $\lambda\delta = 0.1$, 5.1% at $\lambda\delta = 0.2$, and 11% at $\lambda\delta = 0.5$. In the limit of very high electrolyte concentrations, the obtained mobility expression tends to the result derived from the conventional hard step function model. In addition, an analytic expression for the interaction energy between two similar soft plates is derived on the basis of the present soft step function model. The magnitude of the interaction energy is shown to decrease by a factor $1/(1 + \kappa\delta)^2$. Approximate analytic expressions for the interaction energies between two similar soft spheres and between two similar soft cylinders are also derived with the help of Derjaguin's approximation.

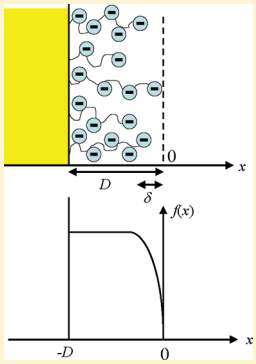

1. INTRODUCTION

A number of theoretical studies[1−27] have been done on the electrophoretic mobility of polyelectrolyte-coated particles, which we term soft particles. These studies are based on the Poisson–Boltzmann equation for the electric potential distribution across the polyelectrolyte layer and the Navier–Stokes equation for the liquid flow inside and outside the polyelectrolyte layer. These theories are also based on the Debye–Bueche model[28] in which the polymer segments are regarded as resistance centers distributed uniformly in the polyelectrolyte layer, exerting frictional forces on the liquid flowing in the polyelectrolyte layer. The electrokinetic theory of soft particles has been employed to analyze experimental data of various polyelectrolyte-coated particles including biological cells.[29−40]

In the above theories[1−27] the polyelectrolyte layer is modeled as a hard step function; that is, the surface charge layer is assumed to have a definite thickness with a uniform segment density distribution. When, however, the polyelectrolyte layer is originated from polymer adsorption, there are some cases in which the effect of the segment density distribution of adsorbed polymers becomes important. Varoqui[41] considered the case where neutral polymers are adsorbed with an exponential segment density distribution. This model should be suitable for θ-solvents, where excluded volume effects are not strong and surface charge densities are moderate. Ohshima[42] extended Varoqui's theory to the case where adsorbed polymers are charged.

Leeuwen and co-workers[43−45] and Duval and co-workers[46,47] have introduced the important concept of "a diffuse soft layer". Duval and Ohshima[34] have presented a novel electrokinetic theory of diffuse soft particles by modeling the polyelectrolyte layer as a sigmoidal function. In the present article as a different model we propose a soft step function model, in which there is the finite maximum segment length. This model differs form any of the above-mentioned three models, that is, the classical hard step function model, Varoqui's exponential function model, and Duval's sigmoidal function model, and should be suitable for particles covered with polymer brush layers. In the present paper on the basis of a soft step function model, we derive approximate analytic expressions for the electrophoretic mobility of a soft particle and the electrostatic interaction energy between two soft particles for the case where the potential is low so that the linearized Poisson–Boltzmann equations can be used.

2. POTENTIAL DISTRIBUTION ACROSS A SOFT PLATE

Consider a soft particle immersed in an aqueous electrolyte solution. The particle consists of an uncharged core covered with an ion-penetrable surface layer of polyelectrolytes of thickness D. We treat the case where the particle size is much larger than the Debye length $1/\kappa$ so that the particle surface can be assumed to be planar. Let the electrolyte be composed of M ionic mobile species of valence z_i, and bulk concentration (number density) n_i (i = 1, 2, ..., M). From the condition of electroneutrality in the bulk solution phase

Special Issue: Herman P. van Leeuwen Festschrift

Received: December 13, 2011
Revised: January 8, 2012
Published: January 8, 2012

dx.doi.org/10.1021/jp212002e | J. Phys. Chem. A 2012, 116, 6473–6480

we have

$$\sum_{i=1}^{M} z_i e n_i = 0 \tag{1}$$

where e is the elementary electric charge. We take an x-axis perpendicular to the particle surface with its origin 0 at the front edge of the surface charge layer so that the region $x > 0$ corresponds to the solution phase (Figure 1). We assume that

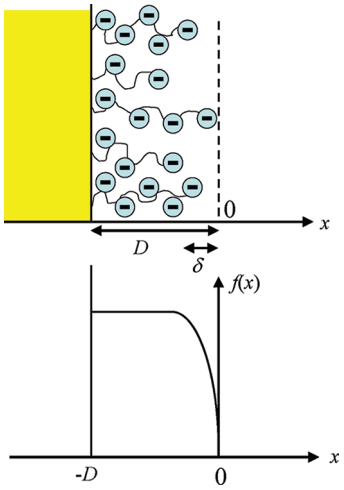

Figure 1. Schematic representation of the surface of a platelike particle covered by an ion-penetrable surface layer of polyelectrolytes (upper) and the segment density distribution modeled as a soft step function (lower).

the polymer segment distribution can be modeled as a soft step function so that its distribution function $f(x)$ is given by

$$f(x) = 1 - \exp(x/\delta) \qquad -D < x < 0 \tag{2}$$

Here δ, which is assumed to satisfy $\delta \ll D$, is a measure of the width of the inhomogeneous distribution of polyelectrolyte segments near the front edge of the polyelectrolyte layer. Equation 2 implies that D corresponds to the maximum segment length. Typically, D is of the order of 10 nm and $\delta \leq 1$ nm. Figure 2 shows $f(x)$ for several values of δ.

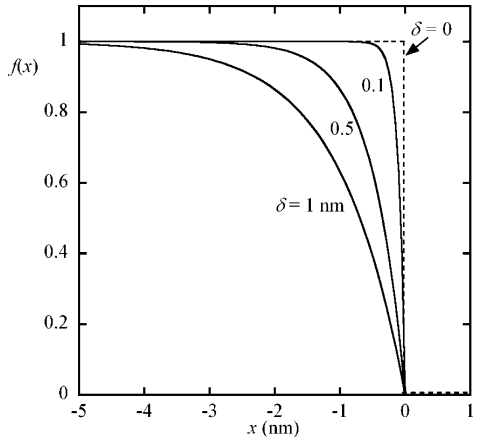

Figure 2. A soft step function $f(x)$ for several values of δ. $f(x)$ with $\delta = 0$ corresponds to the hard step function.

We assume that ionized groups of valence Z are distributed in the polyelectrolyte layer and their density $N(x)$, which is a function of x, is proportional to the distribution function $f(x)$. We also assume that D is much thicker than δ ($\delta \ll D$) so that the density $N(x)$ can be assumed to have a constant value N in the deep inside the surface layer. We may thus write

$$N(x) = Nf(x) = N\{1 - \exp(x/\delta)\} \qquad -D < x < 0 \tag{3}$$

The surface charge density $\rho_{\mathrm{fix}}(x)$ is thus given by

$$\rho_{\mathrm{fix}}(x) = ZeN(x) = ZeNf(x) = Ze \times N\{1 - \exp(x/\delta)\} \qquad -D < x < 0 \tag{4}$$

We assume that the electric potential $\psi(x)$ at position x satisfy the following Poisson–Boltzmann equations:

$$\frac{d^2\psi}{dx^2} = -\frac{\rho_{\mathrm{el}}(x) + \rho_{\mathrm{fix}}(x)}{\varepsilon_r \varepsilon_o} \qquad -D < x < 0 \tag{5}$$

$$\frac{d^2\psi}{dx^2} = -\frac{\rho_{\mathrm{el}}(x)}{\varepsilon_r \varepsilon_o} \qquad x > 0 \tag{6}$$

with

$$\rho_{\mathrm{el}}(x) = \sum_{i=1}^{M} z_i e n_i \exp\left(-\frac{z_i e \psi(x)}{kT}\right) \tag{7}$$

where ε_r is the relative permittivity of the electrolyte solution, ε_o is the permittivity of a vacuum, k is Boltzmann's constant, and T is the absolute temperature. Equation 5 implies that the relative permittivity ε_r takes the same value both inside and outside the surface charge layer.

We assume that the potential $\psi(x)$ is low so that eqs 5–7 can be linearized to give, respectively,

$$\frac{d^2\psi}{dx^2} = \kappa^2\{\psi(x) - \psi_{\mathrm{DON}}(1 - e^{x/\delta})\} \qquad -D < x < 0 \tag{8}$$

$$\frac{d^2\psi}{dx^2} = \kappa^2\psi(x) \qquad x > 0 \tag{9}$$

$$\rho_{\mathrm{el}}(x) = \varepsilon_r \varepsilon_o \kappa^2 \psi(x) \tag{10}$$

where

$$\kappa = \left(\frac{1}{\varepsilon_r \varepsilon_o kT} \sum_{i=1}^{M} z_i^2 e^2 n_i\right)^{1/2} \tag{11}$$

is the Debye–Hückel parameter and ψ_{DON} is the Donnan potential defined by

$$\psi_{\mathrm{DON}} = \frac{ZeN}{\varepsilon_r \varepsilon_o \kappa^2} \tag{12}$$

The boundary conditions for $\psi(x)$ are

$$\left.\frac{d\psi}{dx}\right|_{x=-D} = 0 \tag{13}$$

$$\left.\frac{d\psi}{dx}\right|_{x=0^-} = \left.\frac{d\psi}{dx}\right|_{x=0^+} \tag{14}$$

dx.doi.org/10.1021/jp212002e | J. Phys. Chem. A 2012, 116, 6473–6480

$$\psi(0^-) = \psi(0^+) \tag{15}$$

Equation 13 corresponds to the assumption that the particle core surface is uncharged. The solution to eqs 8 and 9 subject to eqs 13−15 is given by

$$\psi(x) = \frac{ZeN}{\varepsilon_r\varepsilon_o\kappa^2}\left[1 - \frac{e^{\kappa x} + e^{-2\kappa D - \kappa x}}{2(1-\kappa\delta)} + \frac{(\kappa\delta)^2}{1-(\kappa\delta)^2}e^{x/\delta} + \frac{\kappa\delta}{1-(\kappa\delta)^2}e^{-\kappa D - \kappa x - D/\delta}\right] \qquad -D \le x \le 0 \tag{16}$$

$$\psi(x) = \psi_o e^{-\kappa x} \qquad x \ge 0 \tag{17}$$

where

$$\psi_o = \frac{ZeN}{\varepsilon_r\varepsilon_o\kappa^2}\left[1 - \frac{1+e^{-2\kappa D}}{2(1-\kappa\delta)} + \frac{(\kappa\delta)^2}{1-(\kappa\delta)^2} + \frac{\kappa\delta}{1-(\kappa\delta)^2}e^{-\kappa D - D/\delta}\right] \tag{18}$$

is the potential at $x = 0$, which we term the surface potential of the soft particle. For most practical cases, we may assume

$$\kappa D \gg 1 \tag{19}$$

In such cases, eqs 16 and 18 reduce to

$$\psi(x) = \frac{ZeN}{\varepsilon_r\varepsilon_o\kappa^2}\left[1 - \frac{e^{\kappa x}}{2(1-\kappa\delta)} + \frac{(\kappa\delta)^2}{1-(\kappa\delta)^2}e^{x/\delta}\right] \qquad -D \le x \le 0 \tag{20}$$

and

$$\psi_o = \frac{ZeN}{2\varepsilon_r\varepsilon_o\kappa^2(1+\kappa\delta)} = \frac{\psi_{DON}}{2(1+\kappa\delta)} \tag{21}$$

Figure 3 shows the potential distribution across the surface charge layer as a function of κx calculated with eq 20 for several values of $\kappa\delta$.

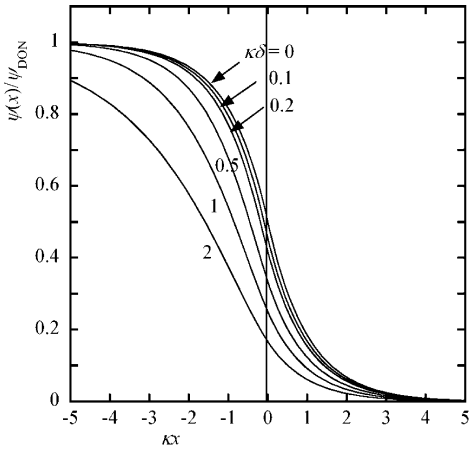

Figure 3. Scaled potential distribution $\psi(x)/\psi_{DON}$ across a soft surface. Calculated with eq 20 for several vales of $\kappa\delta$.

3. ELECTROPHORETIC MOBILITY OF A SOFT PARTICLE

Suppose that the soft particle considered in the previous section is moving with a velocity U in a liquid containing a general electrolyte in an applied electric field E. The electrophoretic mobility μ is given by $\mu = U/E$. Because we treat the case where the particle size is much larger than the Debye length $1/\kappa$, the particle surface can be assumed to be planar and the liquid flow can be assumed to be parallel to the particle surface. We take an x-axis perpendicular to the surface with its origin 0 at the particle surface so that the region $x > 0$ corresponds to the solution phase as in the previous section 2 (Figure 1).

We adopt the model of Debye−Bueche,[28] in which the polymer segments can be treated as resistance centers exerting frictional forces on the liquid flowing in the polyelectrolyte layer. We assume that the frictional coefficient $\tau(x)$, which depends on x, may be expressed as

$$\tau(x) = \tau f(x) = \tau\{1 - \exp(x/\delta)\} \tag{22}$$

τ being a constant. The Navier−Stokes equations for the liquid velocity $u(x)$ (flowing parallel to the particle surface) relative to the particle core surface are

$$\eta\frac{d^2u(x)}{dx^2} - \tau\{1 - \exp(x/\delta)\}u(x) + \rho_{el}(x)E = 0 \qquad -D < x < 0 \tag{23}$$

$$\eta\frac{d^2u(x)}{dx^2} + \rho_{el}(x)E = 0 \qquad x > 0 \tag{24}$$

The boundary conditions for $u(x)$ are

$$u(-D) = 0 \tag{25}$$

$$u(\infty) = -U \tag{26}$$

$$u(0^-) = u(0^+) \tag{27}$$

$$\left.\frac{du}{dx}\right|_{x=0^-} = \left.\frac{du}{dx}\right|_{x=0^+} \tag{28}$$

Equation 25 states that he slipping plane is located at the particle core surface ($x = -D$).

Making the change of variables in eq 23,

$$t = 2\lambda\delta\exp(x/2\delta) \tag{29}$$

with

$$\lambda = (\tau/\eta)^{1/2} \tag{30}$$

we can write eq 23 as

$$\frac{d^2u}{dt^2} + \frac{1}{t}\frac{du}{dt} + \left\{1 - \frac{(2\lambda\delta)^2}{t^2}\right\}u = G(t)E \tag{31}$$

with

$$G(t) = -\frac{4\delta^2}{\eta t^2}\rho_{el}(x) \tag{32}$$

Note that $1/\lambda$ (λ being given by eq 30), which is typically of the order of 1 nm, is often called the softness parameter. In the

dx.doi.org/10.1021/jp212002e | J. Phys. Chem. A 2012, 116, 6473−6480

region $-D < x < 0$, eq 31 can be solved easily to give

$$u(t) = -\frac{\pi}{2}J_{2\lambda\delta}(t)\int_0^t tY_{2\lambda\delta}(t)\,G(t)\,\mathrm{d}t\,E + \frac{\pi}{2}Y_{2\lambda\delta}(t)\int_0^t tJ_{2\lambda\delta}(t)\,G(t)\,\mathrm{d}t\,E + C_1J_{2\lambda\delta}(t) + C_2Y_{2\lambda\delta}(t) \qquad -D < x < 0 \tag{33}$$

where $J_{2\lambda\delta}(t)$ and $Y_{2\lambda\delta}(t)$ are respectively the Bessel functions of the first and second kinds, C_1 and C_2 are constants to be determined, and the lower limit $t = 2\lambda\delta e^{-D/\delta}$ of the integral has been replaced by $t = 0$ with negligible errors for $\delta \ll D$. For $x > 0$, on the other hand, it follows from eq 24 that for the low potential case, by using eq 10, we have

$$u(0^+) = -U + \frac{\varepsilon_r\varepsilon_o}{\eta}\psi_o E \tag{34}$$

$$\left.\frac{\mathrm{d}u}{\mathrm{d}x}\right|_{x=0^+} = -\frac{\varepsilon_r\varepsilon_o}{\eta}\kappa\psi_o E \tag{35}$$

By substituting eqs 33−35 into eqs 27 and 28, we finally find that the electrophoretic mobility $\mu = U/E$ of the soft particle is given by

$$\mu = \frac{ZeN(1+\kappa/\lambda)}{2\eta\kappa^2(1+\kappa\delta)} + \frac{1}{2\lambda\delta J'_{2\lambda\delta}(2\lambda\delta)} \times \int_0^{2\lambda\delta} tJ_{2\lambda\delta}(t)\,G(t)\,\mathrm{d}t \tag{36}$$

with

$$G(t) = \frac{4ZeN\delta^2}{\eta t^2}\left[1 - \frac{1}{2(1-\kappa\delta)}\left(\frac{t}{2\lambda\delta}\right)^{2\kappa\delta} + \frac{(\kappa\delta)^2}{\{1-(\kappa\delta)^2\}}\left(\frac{t}{2\lambda\delta}\right)^2\right] \tag{37}$$

By using the definition of $J_\nu(t)$, i.e.,

$$J_\nu(t) = \left(\frac{t}{2}\right)^\nu \sum_{n=0}^{\infty}\frac{(-1)^n(t/2)^{2n}}{n!\Gamma(\nu+n+1)} \tag{38}$$

where $\Gamma(z)$ is the gamma function, eq 36 can be transformed into

$$\mu = \frac{ZeN}{\eta\lambda^2} + \frac{ZeN(1+\kappa/\lambda)}{2\eta\kappa^2(1+\kappa\delta)} + \frac{ZeN}{\eta\lambda^2}\cdot\frac{(\lambda\delta)^{2\lambda\delta+1}}{J'_{2\lambda\delta}(2\lambda\delta)}\sum_{n=0}^{\infty}\frac{(-1)^n(\lambda\delta)^{2n}}{n!\Gamma(2\lambda\delta+n+1)} \times\left[\frac{1}{\{1-(\kappa\delta)^2\}(\lambda\delta+n+1)} - \frac{1}{2(1-\kappa\delta)(\lambda\delta+\kappa\delta+n)}\right] \tag{39}$$

Here the derivative $J'_{2\lambda\delta}(2\lambda\delta)$ can be rewritten as

$$J'_{2\lambda\delta}(2\lambda\delta) = J_{2\lambda\delta}(2\lambda\delta) - J_{2\lambda\delta+1}(2\lambda\delta) \tag{40}$$

and the following relation has been employed:

$$J'_{2\lambda\delta}(2\lambda\delta) = 2\lambda\delta\int_0^{2\lambda\delta}\left\{\frac{1}{t} - \frac{t}{(2\lambda\delta)^2}\right\}J_{2\lambda\delta}(t)\,\mathrm{d}t \tag{41}$$

Equation 39 as combined with eq 40 is the required expression for the electrophoretic mobility μ of a soft particle with a soft step function. Figure 4 shows μ as a function of κ/λ

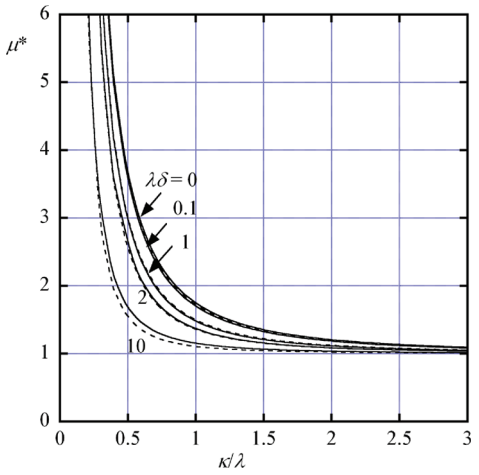

Figure 4. Scaled electrophoretic mobility $\mu^* = \mu/\mu^\infty$ as a function of κ/λ for various values of λd. Calculated with eq 38 as combined with eq 40. Approximate results obtained via eq 44 are also shown as dotted curves.

for various values of $\lambda\delta$. In this limiting case of $\delta \to 0$, eq 38 reduces to

$$\mu = \frac{ZeN}{\eta\lambda^2}\left[1 + \left(\frac{\lambda}{\kappa}\right)^2\left(\frac{1+\lambda/2\kappa}{1+\lambda/\kappa}\right)\right] \tag{42}$$

which agrees with the result for the hard step function model.[6]

We see that the magnitude of μ decreases with increasing $\lambda\delta$. The maximum deviation of the soft step function model from the hard step function model is 2.7% at $\lambda\delta = 0.1$, 5.1% at $\lambda\delta = 0.2$, and 11% at $\lambda\delta = 0.5$. It has been observed that the hard step function model often overestimates the electrophoretic mobility of soft particles especially at low electrolyte concentrations. The present model, which gives smaller mobility values than the hard step function model, is expected to yield better agreement between theory and experiment. We also see that in the limit of large κ, μ tends to μ^∞, where the limiting value μ^∞ is given by

$$\mu^\infty = \frac{ZeN}{\eta\lambda^2} \tag{43}$$

which coincides with the result for the hard step function model. That is, the limiting mobility value μ^∞ is independent of δ.

dx.doi.org/10.1021/jp212002e | J. Phys. Chem. A 2012, 116, 6473−6480

It can be shown that for small $\lambda\delta$, eq 39 can be approximated by the following simple equation:

$$\mu = \frac{ZeN}{\eta\lambda^2}\left[1 + \left(\frac{1}{1+\kappa\delta}\right)\left\{\left(\frac{\lambda}{\kappa}\right)^2\left(\frac{1+\lambda/2\kappa}{1+\lambda/\kappa}\right) + \left(\frac{\lambda/\kappa}{1+\lambda/\kappa}\right)\left(\frac{\lambda\delta}{1+\lambda\delta}\right)\right\}\right] \quad (44)$$

Equation 44 again tends to eq 42 as $\delta \to 0$. Some results of the calculation via eq 44 are also shown in Figure 4, showing excellent agreement with the exact results obtained from eq 39.

4. ELECTROSTATIC INTERACTION BETWEEN TWO SOFT PARTICLES

Consider the electrostatic interaction between two parallel dissimilar soft plates 1 and 2, both being similar to those treated in the previous sections. The plates are separated by h as shown in Figure 5. We take an x-axis perpendicular to the plates with its origin at the front edge of the surface charge layer of plate 1. Plates 1 and have surface charge layers of thicknesses D_1 and D_2, respectively. The segment density distributions for plates 1 and 2 are given by the following soft step functions:

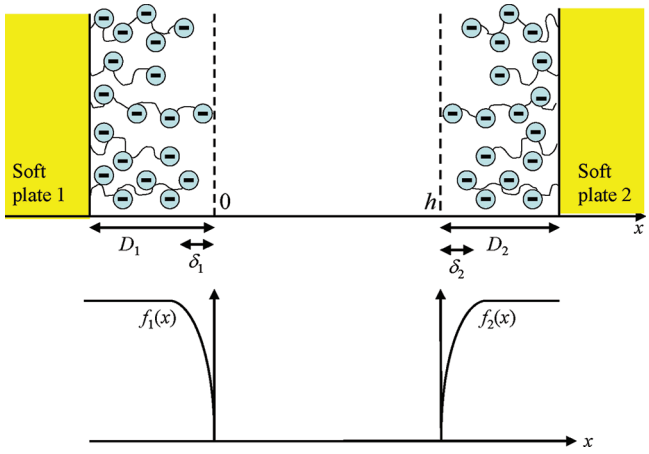

Figure 5. Schematic representation of the interaction between two parallel soft plates 1 and 2 covered by surface charge layers of thicknesses D_1 and D_2 at separation h. The polymer segment distributions of plates 1 and 2 are modeled as soft step functions $f_1(x)$ and $f_2(x)$, respectively.

$$f_1(x) = 1 - \exp(x/\delta_1) \qquad -D_1 < x < 0 \quad (45)$$

$$f_2(x) = 1 - \exp((h-x)/\delta_2) \qquad h < x < h + D_2 \quad (46)$$

where δ_1 corresponds to the width of the inhomogeneous distribution of polyelectrolyte segments near the front edge of the polyelectrolyte layer of plate 1 and δ_2 to that for plate 2. We assume that ionized groups of valence Z_1 are distributed at a uniform density N_1 in the deep inside the surface layer of plate 1 and let Z_2 and N_2 be corresponding quantities for plate 2.

For the low potential case the Poisson–Boltzmann equations

$$\frac{d^2\psi}{dx^2} = \kappa^2[\psi(x) - \psi_{DON1}\{1 - \exp(x/\delta_1)\}] \qquad -D < x < 0 \quad (47)$$

$$\frac{d^2\psi}{dx^2} = \kappa^2\psi(x) \qquad 0 < x < h \quad (48)$$

$$\frac{d^2\psi}{dx^2} = \kappa^2[\psi(x) - \psi_{DON1}\{1 - \exp((h-x)/\delta_2)\}] \qquad h < x < h + D_2 \quad (49)$$

It can be shown that, when $\kappa D_1 \gg 1$ and $\kappa D_2 \gg 1$, the solution $\psi(x)$ to eqs 47–49 subject to the appropriate boundary conditions is given by

$$\psi(x) = \frac{Z_1eN_1}{\varepsilon_r\varepsilon_o\kappa^2}\left[1 - \frac{e^{\kappa x}}{2(1-\kappa\delta_1)} + \frac{(\kappa\delta_1)^2 e^{x/\delta_1}}{1-(\kappa\delta_1)^2}\right] + \psi_{o2}e^{-\kappa(h-x)} \qquad -D_1 < x < 0 \quad (50)$$

$$\psi(x) = \psi_{o1}e^{-\kappa x} + \psi_{o2}e^{-\kappa(h-x)} \qquad 0 < x < h \quad (51)$$

$$\psi(x) = \psi_{o1}e^{-\kappa x} + \frac{Z_2eN_2}{\varepsilon_r\varepsilon_o\kappa^2}\left[1 - \frac{e^{\kappa(h-x)}}{2(1-\kappa\delta_2)} + \frac{(\kappa\delta_2)^2 e^{(h-x)/\delta_1}}{1-(\kappa\delta_2)^2}\right] \qquad h < x < h + D_2 \quad (52)$$

with

$$\psi_{o1} = \frac{Z_1eN_1}{2\varepsilon_r\varepsilon_o\kappa^2(1+\kappa\delta_1)} = \frac{\psi_{DON1}}{2(1+\kappa\delta_1)} \quad (53)$$

$$\psi_{o2} = \frac{Z_2eN_2}{2\varepsilon_r\varepsilon_o\kappa^2(1+\kappa\delta_2)} = \frac{\psi_{DON2}}{2(1+\kappa\delta_2)} \quad (54)$$

$$\psi_{DON1} = \frac{Z_1eN_1}{\varepsilon_r\varepsilon_o\kappa^2} \quad (55)$$

$$\psi_{DON2} = \frac{Z_2eN_2}{\varepsilon_r\varepsilon_o\kappa^2} \quad (56)$$

where ψ_{o1} and ψ_{o2} are respectively the unperturbed surface potentials of plates 1 and 2, and ψ_{DON1} and ψ_{DON2} are, respectively, the Donnan potentials in the surface charge layers of plates 1 and 2. Figure 6 show how $\psi(x)$ depends on the value of $\kappa\delta$. It is seen that the potential in the region deep inside the surface charge layer practically equals the Donnan potential ψ_{DON}.

The force $P(h)$ of the electrostatic interaction per unit area between plates 1 and 2 at separation h can be calculated by integrating the osmotic pressure and the Maxwell stress over an arbitrary surface enclosing one of plates 1 and 2.[48] That is,

$$P(h) = \frac{1}{2}\varepsilon_r\varepsilon_o\left[\kappa^2\psi^2(x') - \left(\frac{d\psi}{dx}\bigg|_{x=x'}\right)^2\right] \quad (57)$$

dx.doi.org/10.1021/jp212002e | J. Phys. Chem. A 2012, 116, 6473–6480

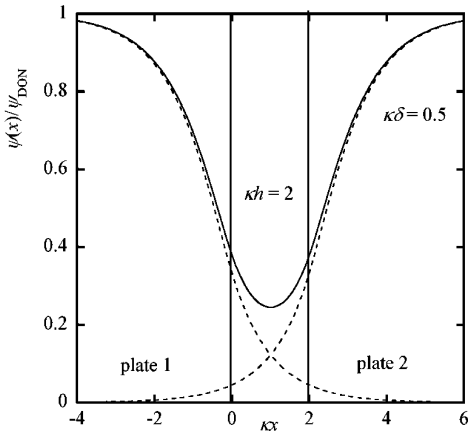

Figure 6. Scaled potential distribution $\psi(x)/\psi_{DON}$ across two interacting similar soft plates. Calculated with eqs 48−50. The dotted curves are the scaled unperturbed potential distribution at $\kappa h = \infty$.

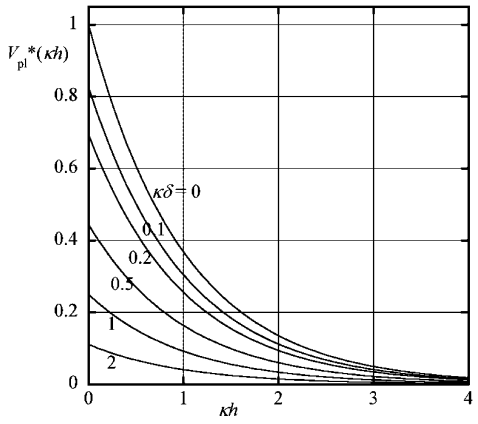

Figure 7. Reduced interaction energy $V^*(\kappa h) = V(\kappa h)/((ZeN)^2/2\varepsilon_r\varepsilon_o\kappa^3)$ per unit area between two similar parallel plates as a function of reduced separation κh for several values of $\kappa\delta$. Calculated with eq 61.

where x' is an arbitrary point in the region $0 \le x \le h$. By substituting eq 51 into eq 57, we obtain

$$P(h) = \frac{(Z_1eN_1)(Z_2eN_2)}{2\varepsilon_r\varepsilon_o\kappa^2(1+\kappa\delta_1)(1+\kappa\delta_2)}e^{-\kappa h} \quad (58)$$

From eq 58 we obtain the following expression for the potential energy $V_{pl}(h)$ of the electrostatic interaction per unit area between two dissimilar soft plates 1 and 2 at separation h, which is related to $P(h)$ by $P(h) = -dV(h)/dh$,

$$V_{pl}(h) = \frac{(Z_1eN_1)(Z_2eN_2)}{2\varepsilon_r\varepsilon_o\kappa^3(1+\kappa\delta_1)(1+\kappa\delta_2)}e^{-\kappa h} \quad (59)$$

In the limit of $\kappa\delta_1 \to 0$ and $\kappa\delta_2 \to 0$, eq 59 tends to

$$V_{pl}(h) = \frac{(Z_1eN_1)(Z_2eN_2)}{2\varepsilon_r\varepsilon_o\kappa^3}e^{-\kappa h} \quad (60)$$

which agrees with the result for the hard step function model.[48,49] For the special case of two similar soft plates ($N_1 = N_2 = N$, $Z_1 = Z_2 = Z$), eq 60 reduces to

$$V_{pl}(h) = \frac{(ZeN)^2}{2\varepsilon_r\varepsilon_o\kappa^3(1+\kappa\delta)^2}e^{-\kappa h} \quad (61)$$

We see that the magnitude of the interaction energy decreases by a factor of $1/\{(1+\kappa\delta_1)(1+\kappa\delta_2)\}$ for dissimilar plates and $1/(1+\kappa\delta)^2$ for similar plates by taking into account the effect of the polymer segment distribution. Figure 7 shows how $V(h)$ depends on $\kappa\delta$.

With help of Derjaguin's method[50,51] it is possible to derive approximate analytic expressions for the interaction energy between two soft spheres or cylinders. It follows from Derjaguin's method that the interaction energy $V_{sp}(H)$ between two spheres of radii a_1 and a_2 at separation H (Figure 8) can be calculated form the corresponding interaction energy $V_{pl}(h)$ per unit area between two parallel plates via

$$V_{sp}(H) = \frac{2\pi a_1a_2}{a_1+a_2}\int_H^\infty V_{pl}(h)\,dh \quad (62)$$

For two parallel cylinders of radii a_1 and a_2 at separation H (Figure 9), the interaction energy per unit length is

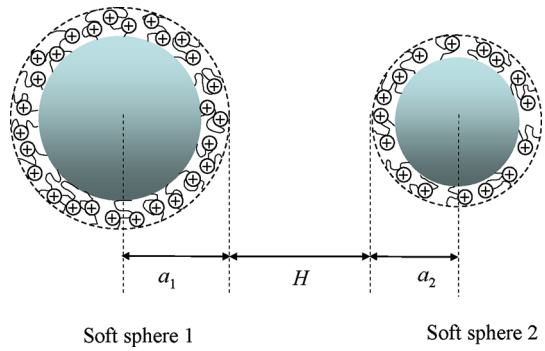

Figure 8. Interaction between two spheres 1 and 2 of radii a_1 and a_2, respectively.

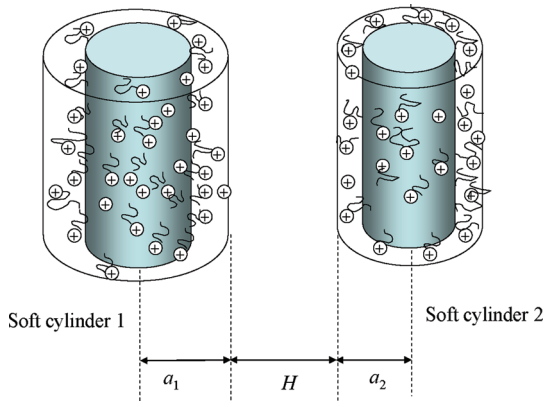

Figure 9. Interaction between two parallel soft cylinders 1 and 2 of radii a_1 and a_2, respectively.

given by[52,53]

$$V_{cy\parallel}(H) = \sqrt{\frac{2a_1a_2}{a_1+a_2}}\int_H^\infty V_{pl}(h)\frac{dh}{\sqrt{h-H}} \quad (63)$$

For two crossed cylinders of radii a_1 and a_2 at separation H, as shown in Figure 10, the interaction energy is given by[52,53]

$$V_{cy\perp}(H) = 2\pi\sqrt{a_1a_2}\int_H^\infty V_{pl}(h)\,dh \quad (64)$$

dx.doi.org/10.1021/jp212002e | J. Phys. Chem. A 2012, 116, 6473−6480

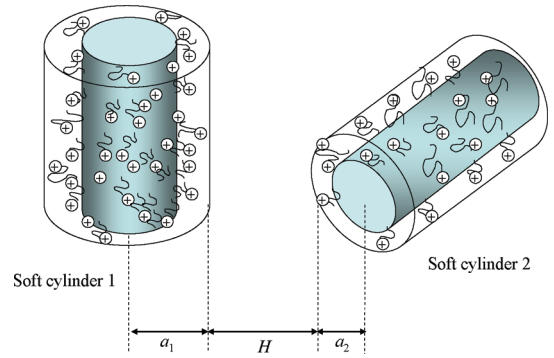

Figure 10. Interaction between two crossed soft cylinders 1 and 2 of radii a_1 and a_2, respectively.

By substituting eq 60 into eqs 62−64, one can calculate the interaction energies between two soft spheres, two parallel soft cylinders, and two crossed soft cylinders. The results are listed below.

$$V_{sp}(H) = \left(\frac{\pi a_1 a_2}{a_1 + a_2}\right)\frac{(Z_1eN_1)(Z_2eN_2)}{\varepsilon_r\varepsilon_o\kappa^4(1 + \kappa\delta_1)(1 + \kappa\delta_2)}e^{-\kappa H} \quad (65)$$

$$V_{cy\parallel}(H) = \sqrt{\frac{2\pi a_1 a_2}{a_1 + a_2}} \times \frac{(Z_1eN_1)(Z_2eN_2)}{2\varepsilon_r\varepsilon_o\kappa^{7/2}(1 + \kappa\delta_1)(1 + \kappa\delta_2)}e^{-\kappa H} \quad (66)$$

$$V_{cy\perp}(H) = \pi\sqrt{a_1 a_2}\frac{(Z_1eN_1)(Z_2eN_2)}{\varepsilon_r\varepsilon_o\kappa^4(1 + \kappa\delta_1)(1 + \kappa\delta_2)}e^{-\kappa H} \quad (67)$$

In the limiting case of $\kappa\delta_1 \to 0$ and $\kappa\delta_2 \to 0$, eqs 65−67 tend to

$$V_{sp}(H) = \left(\frac{\pi a_1 a_2}{a_1 + a_2}\right)\frac{(Z_1eN_1)(Z_2eN_2)}{\varepsilon_r\varepsilon_o\kappa^4}e^{-\kappa H} \quad (68)$$

$$V_{cy\parallel}(H) = \sqrt{\frac{2\pi a_1 a_2}{a_1 + a_2}}\frac{(Z_1eN_1)(Z_2eN_2)}{2\varepsilon_r\varepsilon_o\kappa^{7/2}}e^{-\kappa H} \quad (69)$$

$$V_{cy\perp}(H) = \pi\sqrt{a_1 a_2}\frac{(Z_1eN_1)(Z_2eN_2)}{\varepsilon_r\varepsilon_o\kappa^4}e^{-\kappa H} \quad (70)$$

which agree with the results for the hard step function model.[15,53,54] Equations 68−70 are derived, of course, also by substituting eq 60 into eqs 62−64, respectively.

5. CONCLUSIONS

We have developed a theory of electrostatics and electrokinetics of soft particles in an electrolyte solution. The soft particle consists of the particle core covered by an ion-penetrable surface layer of polyelectrolytes. The polyelectrolyte layer is modeled as a soft step function given by eq 2. The present model is different from an exponential function model and a sigmoidal function model in that in the present model the surface layer has a *finite* thickness D (with the inhomogeneous segment distribution of width δ) whereas in the other two models the density distribution extends *infinitely*. Thus, in the present model, as in the traditional hard step function model, it is possible to define the distance between two soft particles so that expressions for the interaction force and energy between the soft particles can easily be derived. We have derived analytic expressions for the electrophoretic mobility of the soft particle (eqs 39 and 44) and for the interaction energy between two soft particle of various geometry including parallel soft plates (eq 59), two spheres (eq 65), two parallel cylinders (eq 66), and two crossed cylinders (eq 67). The magnitudes of the electrophoretic mobility and the interaction energy becomes smaller than those for the classical hard step function model.

AUTHOR INFORMATION

Corresponding Author

*Fax: +81-4-7121-3661. E-mail: ohshima@rs.noda.tus.ac.jp.

REFERENCES

(1) Donath, E.; Pastuschenko, V. *Bioelectrochem. Bioenerg.* **1980**, *7*, 31.
(2) Wunderlich, R. W. *J. Colloid Interface Sci.* **1982**, *88*, 385.
(3) Levine, S.; Levine, M.; Sharp, K. A.; Brooks, D. E. *Biophys. J.* **1983**, *42*, 127.
(4) Sharp, K. A.; Brooks, D. E. *Biophys. J.* **1985**, *47*, 563.
(5) Donath, E.; Voigt, A. *J. Colloid Interface Sci.* **1986**, *109*, 122.
(6) Ohshima, H. *J. Colloid Interface Sci.* **1994**, *163*, 474.
(7) Ohshima, H. *Colloids Surf. A: Physicochem. Eng. Asp.* **1995**, *103*, 249.
(8) Ohshima, H. *Electrophoresis* **1995**, *16*, 136.
(9) Ohshima, H. *Adv. Colloid Interface Sci.* **1995**, *62*, 189.
(10) Ohshima, H. *J. Colloid Interface Sci.* **2000**, *228*, 190.
(11) Saville, D. A. *J. Colloid Interface Sci.* **2000**, *222*, 137.
(12) Ohshima, H. *J. Colloid Interface Sci.* **2001**, *233*, 142.
(13) Hill, R. J.; Saville, D. A.; Russel, W. B. *J. Colloid Interface Sci.* **2003**, *258*, 56.
(14) Hill, R. J.; Saville, D. A.; Russel, W. B. *J. Colloid Interface Sci.* **2003**, *263*, 478.
(15) Lopez-Garcia, J. J.; Grosse, C.; Horno, J. *J. Colloid Interface Sci.* **2003**, *265*, 327.
(16) Dukhin, S. S.; Zimmermann, R.; Werner, C. *J. Colloid Interface Sci.* **2004**, 274.
(17) Ohshima, H. *Colloid Polym. Sci.* **2005**, *283*, 819.
(18) Hill, R. J.; Saville, D. A. *Colloids Surfaces A: Physicochem. Eng. Asp.* **2005**, *267*, 31.
(19) Dukhin, S. S.; Zimmermann, R.; Werner, C. *Adv. Colloid Interface Sci.* **2006**, *122*, 93.
(20) Ohshima, H. *Electrophoresis* **2006**, *27*, 526.
(21) Ohshima, H. *Colloid Polym. Sci.* **2006**, *285*, 1411.
(22) Ohshima, H. *Theory of Colloid and Interfacial Electric Phenomena*; Elsevier: Amsterdam, 2006.
(23) Ohshima, H. *Sci. Technol. Adv. Mater.* **2009**, *10*, 063001.
(24) Ahualli, S.; Jiménez, M. L.; Carrique, F.; Delgado, A. V. *Langmuir* **2009**, *25*, 1986.
(25) Ohshima, H. *Biophysical Chemistry of Biointerfaces*; John Wiley & Sons: Hoboken, 2010.
(26) Ohshima, H. *J. Colloid Interface Sci.* **2010**, *349*, 641.
(27) Ohshima, H. *Colloids Surfaces A: Physicochem. Eng. Asp.* **2011**, *376*, 72.
(28) Debye, P.; Bueche, A. *J. Chem. Phys.* **1948**, *16*, 573.
(29) Ohshima, H.; Makino, K.; Kato, T.; Fujimoto, K.; Kondo, T.; Kawaguchi, H. *J. Colloid Interface Sci.* **1993**, *159*, 512.
(30) Makino, K.; Taki, T.; Ogura, M.; Handa, S.; Nakajima, M.; Kondo, T.; Ohshima, H. *Biophys. Chem.* **1993**, *47*, 261.
(31) Mazda, T.; Makino, K.; Ohshima, H. *Colloids Surf. B.* **1995**, *5*, 75. Mazda, T.; Makino, K.; Ohshima, H. Erratum. *Colloids Surf. B.* **1998**, *10*, 303.
(32) Takashima, S.; Morisaki, H. *Colloids Surf. B: Biointerfaces* **1997**, *9*, 205.

(33) Bos, R.; van der Mei, H. C.; Busscher, H. J. *Biophys. Chem.* **1998**, *74*, 251.
(34) Larsson, A.; Rasmusson, M.; Ohshima, H. *Carbohydr. Res.* **1999**, *317*, 223.
(35) Morisaki, H.; Nagai, S.; Ohshima, H.; Ikemoto, E; Kogure, K. *Microbiology* **1999**, *145*, 2797.
(36) Rasmusson, M.; Vincent, B.; Marston, N. *Colloid Polym. Sci.* **2000**, *278*, 253.
(37) Hayashi, H.; Tsuneda, S.; Hirata, A.; Sasaki, H. *Colloids Surf. B: Biointerfaces* **2001**, *22*, 149.
(38) Garcia-Salinas, M. J.; Romero-Cano, M. S.; de las Nieves, F. J. *Prog. Colloid Polym. Sci.* **2001**, *118*, 180.
(39) Kiers, P. J. M.; Bos, R.; van der Mei, H. C.; Busscher, H. J. *Microbiology* **2001**, *147*, 757.
(40) Molina-Bolivar, J. A.; Galisteo-Gonzalez, F.; Hidalgo-Alvalez, R. *Colloids Surf. B: Biointerfaces* **2001**, *21*, 125.
(41) Varoqui, R. *Nouv. J. Chim.* **1982**, *6*, 187.
(42) Ohshima, H. *J. Colloid Interface Sci.* **1997**, *185*, 269.
(43) Duval, J. F. L.; van Leeuwen, H. P. *Langmuir* **2004**, *20*, 10324.
(44) Duval, J. F. L. *Langmuir* **2005**, *21*, 3247.
(45) Yezek, L. P.; Duval, J. F. L.; van Leeuwen, H. P. *Langmuir* **2005**, *21*, 6260.
(46) Duval, J. F. L.; Ohshima, H. *Langmuir* **2006**, *22*, 3533.
(47) Duval, J. F. L.; Gaboriaud, F. *Curr. Opin. Colloid Interface Sci.* **2010**, *15*, 184.
(48) Ohshima, H.; Makino, K; Kondo, T. *J. Colloid Interface Sci.* **1987**, *116*, 196.
(49) Ohshima, H.; Kondo, T. *J. Theor. Biol.* **1987**, *128*, 187.
(50) Derjaguin, B. V. *Kolloid Z.* **1934**, *69*, 155.
(51) Derjaguin, B. V. *Theory of Stability of Colloids and Thin Films*; Consultants Bureau,: New York, London, 1989.
(52) Sparnaay, M. J. *Recueil* **1959**, *712*, 6120.
(53) Ohshima, H.; Hyono, A. *J. Colloid Interface Sci.* **2009**, *202*, 208.
(54) Ohshima, H. *J. Colloid Interface Sci.* **2008**, *328*, 3.